Int. J. Heat Mass Transfer. Vol. 12, pp. 731–737

0017-9310/79/0501-0731 $02.00/0

INFLUENCE OF SLIP VELOCITY AT A MEMBRANE SURFACE ON ULTRAFILTRATION PERFORMANCE—II. TUBE FLOW SYSTEM

RAJINDAR SINGH and ROBERT L. LAURENCE
Department of Chemical Engineering, University of Massachusetts, Amherst, MA 01003, U.S.A.

(*Received* 1 *August* 1977 *and in revised form* 24 *August* 1978)

Abstract—The effect of slip velocity at a membrane surface is studied in detail for a tubular membrane system. A second-order perturbation solution of the equations of motion is found to be very satisfactory. The results are compared with those of the channel flow system reported earlier. As in the case of channel flow system, the effect of slip coefficient on concentration polarization is identical to that of Péclet number—it augments diffusive transport of solute molecules from the membrane surface to the bulk solution.

NOMENCLATURE

A_j, B_j, E_j, F_j, coefficients in the matrix equation;
c, solute concentration;
c_0, inlet solute concentration;
c_w, solute concentration at membrane surface;
$\bar{c}$, $c_0/(1-\zeta)$, mixing-cup average solute concentration;
C, c/c_0;
C_p, $c_w/\bar{c}-1$, concentration polarization;
$(C_p)\theta/(C_p)_{\theta=0}$, normalized concentration polarization;
D, solute diffusivity;
k, membrane permeability;
p, pressure in the tube;
Pe, $1/\alpha_1$, Péclet number;
r, distance normal to phase boundary;
r_w, tube radius;
Re, $2\bar{u}_0 r_w/\nu$, Reynolds number;
Re_w, $2v_w r_w/\nu$, wall Reynolds number;
u, velocity component in x-direction;
$\bar{u}_0$, average velocity over the tube at tube inlet;
$\bar{u}$, average velocity over the tube at a given value of x;
U, $u/\bar{u}_0$;
u_s, $(u/\bar{u})_{\eta=1}$, normalized slip velocity;
v, velocity component in r-direction;
v_w, velocity of fluid through membrane;
V, v/v_w;
x, axial distance from tube entrance.

Greek symbols

α_1, $2D/r_w v_w$, normalized diffusion coefficient;
α, surface characteristic of membrane;
ζ, $2v_w x/\bar{u}_0 r_w = 2Re_w x/Re r_w$, fraction of water removed at a given value of x;
η, $(r/r_w)^2$;
θ, $k^{1/2}/\alpha r_w$, slip coefficient;
ν, kinematic viscosity;
ρ, solution density;
ψ, stream function.

Superscripts

i, ii, iii, iv, first, second, third and fourth-order derivatives.

1. INTRODUCTION

THE EFFECT of slip velocity at the membrane surface on concentration polarization has been studied in detail for a channel flow ultrafiltration system by Singh and Laurence [4]. In the present study, this work has been extended to a tubular flow system, since most of the commercially available ultrafiltration systems are tubular in structure.

Brian [2] studied concentration polarization in tubular membranes, assuming fully-developed flow at the tube entrance, for a limited number of values of the normalized diffusion coefficient. In contrast to his channel flow study he obtained only an infinite-series solution. In this study, the diffusion equation is solved by a finite difference technique and the results compared with those of Brian, assuming slip velocity at the membrane surface.

In order to solve the diffusion equation in the concentrated boundary layer, the velocity field must be specified. Sparrow *et al.* [5] studied tube flows with surface mass transfer and slip velocity. They solved the equations of motion employing an indirect numerical method. Such a method has its obvious drawbacks. To circumvent these drawbacks, the equations of motion are solved by a second-order perturbation method and the two results compared. The results of the solutions are discussed in Section 4 and the conclusions are presented in Section 5.

As in the case of channel flow system, the effect of slip velocity on velocity profiles and concentration polarization has been studied. The ramifications of the slip velocity on predicting flux rates have also been examined.

2. FORMULATION OF THE PROBLEM

2.1. *The equations of motion*

A macromolecular solution is considered to be

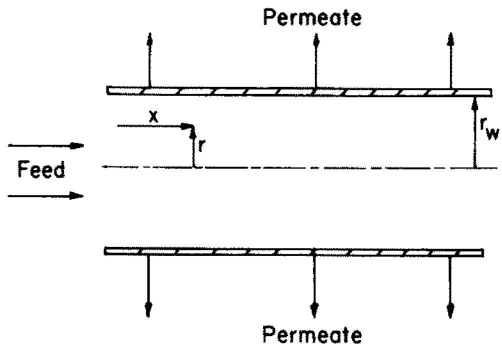

FIG. 1. Tubular membrane.

flowing in a tubular membrane ultrafilter, as shown in Fig. 1. It is assumed that the fluid is incompressible and the operation is steady-state. The flow is assumed to be fully-developed at the tube entrance. Then, the equations of linear momentum and continuity in cylindrical co-ordinates are

$$u\frac{\partial v}{\partial x}+v\frac{\partial v}{\partial r}=-\frac{1}{\rho}\frac{\partial p}{\partial r}+\nu\left\{\frac{\partial}{\partial r}\left[\frac{1}{r}\frac{\partial}{\partial r}(rv)\right]+\frac{\partial^2 v}{\partial x^2}\right\}, \tag{1}$$

$$u\frac{\partial u}{\partial x}+v\frac{\partial u}{\partial r}=-\frac{1}{\rho}\frac{\partial p}{\partial x}+\nu\left[\frac{1}{r}\frac{\partial}{\partial r}\left(r\frac{\partial u}{\partial r}\right)+\frac{\partial^2 u}{\partial x^2}\right] \tag{2}$$

and

$$\frac{\partial u}{\partial x}+\frac{1}{r}\frac{\partial}{\partial r}(rv)=0. \tag{3}$$

The boundary conditions are

$$u(x, r_w)=-\frac{k^{1/2}}{\alpha}\left(\frac{\partial u}{\partial r}\right), \tag{4}$$

$$\left(\frac{\partial u}{\partial r}\right)_{r=0}=0, \tag{5}$$

$$v(x, 0)=0, \tag{6}$$

$$v(x, r_w)=v_w. \tag{7}$$

Equation (4) is the slip-flow boundary condition of Beavers and Joseph which has been discussed earlier [4]. According to this model, the slip velocity at the membrane surface is proportional to the shear rate at the permeable boundary. When $k=0$, equation (4) reduces to the no-slip condition appropriate to a solid wall. Equation (7) is the condition for constant permeation flux along the length of the tube.

For a two-dimensional incompressible flow a stream function $\psi(x, \eta)$ exists such that

$$u(x, \eta)=\frac{2}{r_w^2}\frac{\partial \psi}{\partial \eta}, \tag{8}$$

$$v(x, \eta)=-\frac{1}{\eta^{1/2} r_w}\frac{\partial \psi}{\partial x}, \tag{9}$$

where

$$\eta=\left(\frac{r}{r_w}\right)^2 \tag{10}$$

and the continuity equation (3) is satisfied.

A suitable choice of stream function is

$$\psi(x, \eta)=\frac{r_w}{2}\left[r_w \bar{u}_0-2v_w x\right]F(\eta). \tag{11}$$

Combining equations (8), (9) and (11) yields the following expressions for velocity components:

$$u(x, \eta)=\left[\bar{u}_0-\frac{2v_w x}{r_w}\right]F^{i}(\eta), \tag{12}$$

$$v(\eta)=\frac{v_w F(\eta)}{\eta^{1/2}}. \tag{13}$$

All the unknowns are lumped together in $F(\eta)$, a function yet to be determined. The velocity component v, becomes a function of η only because of the assumption of constant permeation flux v_w. Equations (1) and (2) with the definitions of equations (12) and (13) can be used to yield the following result:

$$\eta F^{iv}+2F^{iii}+\frac{Re_w}{4}\left(F^{i}F^{ii}-FF^{iii}\right)=0. \tag{14}$$

The new set of boundary conditions is obtained by substituting equations (12) and (13) in equations (4)–(7). Thus,

$$F^{i}(1)+2\theta F^{ii}(1)=0, \tag{15}$$

$$\eta^{1/2}F^{ii}(\eta)\rightarrow 0, \quad \text{as } \eta\rightarrow 0, \tag{16}$$

$$F(0)=0, \tag{17}$$

$$F(1)=1, \tag{18}$$

where, θ is the slip coefficient equal to $k^{1/2}/\alpha r_w$. Equations (14)–(18) are solved in Section 3.1.

2.2. *The diffusion equation*

The assumptions used to solve the diffusion equation in the concentrated boundary layer are as follows: (1) uniform solute concentration over the tube cross-section at the inlet, (2) a developing concentration profile along the length of the tube, (3) steady-state operation, (4) convection of solute molecules in the axial and radial directions, (5) diffusive transport of solute in the axial and radial directions. It can be shown that diffusion in the axial direction is negligible [4]. On the basis of these assumptions, the appropriate diffusion equation (in dimensionless form) is

$$U\frac{\partial C}{\partial \zeta}+(V\eta^{1/2}-\alpha_1)\frac{\partial C}{\partial \eta}=\alpha_1\eta\frac{\partial^2 C}{\partial \eta^2}. \tag{19}$$

The boundary conditions are

$$C(0, \eta)=1, \tag{20}$$

$$\eta^{1/2}\left(\frac{\partial C}{\partial \eta}\right)\rightarrow 0, \quad \text{as } \eta\rightarrow 0, \tag{21}$$

$$C(\zeta, 1)=\alpha_1\left(\frac{\partial C}{\partial \eta}\right)_{\eta=1}, \tag{22}$$

where

$$U = \frac{u}{\bar{u}_0},\quad V = \frac{v}{v_w},\quad C = \frac{c}{c_0},\quad \alpha_1 = \frac{2D}{v_w r_w},$$
$$\eta = \left(\frac{r}{r_w}\right)^2,\quad \zeta = \frac{2v_w x}{\bar{u}_0 r_w} = \frac{2Re_w x}{Re r_w}. \qquad (23)$$

Equation (22) is the steady-state, gel-polarization model [1]. Equations (19)–(22) are solved in Section 3.2 using the velocity field obtained in Section 3.1.

3. METHODS OF SOLUTION

3.1. *The perturbation solution*

The fourth-order, nonlinear equation (14) was solved by Sparrow *et al.* [5] using an indirect numerical approach. The nature of the solution was thus lost. To circumvent this limitation, equation (14) is solved by a perturbation method. The solution of equation (14) for small values of Re_w may be expressed in the form of a power series as

$$F(\eta) = F_0(\eta) + F_1(\eta)Re_w + F_2(\eta)Re_w^2 + F_3(\eta)R_w^3 + \ldots, \qquad (24)$$

where F_n's are taken to be independent of Re_w.

Combining equations (14) and (24) and equating terms of like powers in Re_w leads to the following set of equations where we let $q = F_j^{iii}$:

$$\eta \frac{dq}{d\eta} + 2q = f_j(\eta), \qquad (25)$$

zero-order:

$$f_0(\eta) = 0, \qquad (26)$$

first-order:

$$f_1(\eta) = F_0 F_0^{iii} - F_0^{i} F_0^{ii}, \qquad (27)$$

second-order:

$$f_2(\eta) = F_1 F_0^{iii} + F_0 F_1^{iii} - F_1^{i} F_0^{ii} - F_0^{i} F_1^{ii}. \qquad (28)$$

The boundary conditions can be stated as

$$F_n^{i}(1) + 2\theta F_n^{ii}(1) = 0, \qquad (29)$$

$$\eta^{1/2} F_n^{ii}(\eta) \to 0, \quad \text{as } \eta \to 0, \qquad (30)$$

$$F_n(0) = 0, \qquad (31)$$

$$\left.\begin{array}{l} F_0(1) = 0, \\ F_n(1) = 1, \end{array}\right. \quad \text{for } n \geq 1. \qquad (32)$$

Equations (26)–(28) with (25) are solved to obtain a second-order perturbation solution to give

$$F(\eta) = E(M\eta - \eta^2) + Re_w Q(G\eta - H\eta^2 + P\eta^3 - \eta^4) + Re_w^2 T(H_1\eta - G_1\eta^2 + E_1\eta^3 - D_1\eta^4 + C_1\eta^5 - A_1\eta^6), \qquad (33)$$

where $E, M, Q, G, H, P, T, H_1, G_1, E_1, D_1, C_1$ and A_1 are functions of θ and are defined in the Appendix.

The velocity profiles are obtained by substituting equation (33) in equations (12) and (13). Hence

$$U = [1-\zeta][E(M-2\eta) + Re_w Q(G - 2H\eta + 3P\eta^2 - 4\eta^3) + Re_w^2 T(H_1 - 2G_1\eta + 3E_1\eta^2 - 4D_1\eta^3 + 5C_1\eta^4 - 6A_1\eta^5)], \qquad (34)$$

$$V = E(M\eta^{1/2} - \eta^{3/2}) + Re_w Q(G\eta^{1/2} - H\eta^{3/2} + P\eta^{5/2} - \eta^{7/2}) + Re_w^2 T(H_1\eta^{1/2} - G_1\eta^{3/2} + E_1\eta^{5/2} - D_1\eta^{7/2} + C_1\eta^{9/2} - A_1\eta^{11/2}). \qquad (35)$$

The normalized axial velocity component $u/\bar{u}$, is

$$\frac{u}{\bar{u}} = E(M - 2\eta) + Re_w Q(G - 2H\eta + 3P^2\eta - 4\eta^3) + Re_w^2 T(H_1 - 2G_1\eta + 3E_1\eta^2 - 4D_1\eta^3 + 5C_1\eta^4 - 6A_1\eta^5), \qquad (36)$$

where

$$\bar{u} = \frac{\int_0^{2\pi}\int_{\eta=0}^{\eta=1} u(\eta)\,d\eta\,d\theta}{\int_0^{2\pi}\int_{\eta=0}^{\eta=1} d\eta\,d\theta} = 1 - \zeta. \qquad (37)$$

3.2. *The finite difference solution*

The velocity field having been obtained, the diffusion equation (19), is solved by a finite difference scheme implicit in η. The details are outlined in the Appendix.

4. RESULTS AND DISCUSSION

4.1. *Velocity profiles*

A second-order perturbation solution of the velocity field is obtained as given by equations (34)–(36). Typical velocity profiles are plotted for parametric values of the slip coefficient θ equal to 0 (no slip), 0.1 and 0.5 and the wall Reynolds number Re_w equal to 2.0 in Fig. 2. It is seen that the

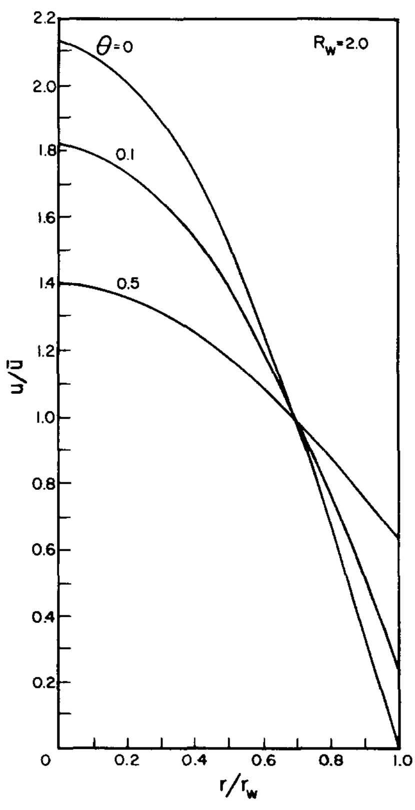

FIG. 2. Velocity profiles for $Re_w = 2.0$ for tube flow.

normalized slip velocity u_s increases with θ, as u_s increases with θ, the wall shear rate decreases and the profiles become flatter approaching those for plug flow. As Re_w increases, u_s decreases and $(u/\bar{u})$max increases. This behavior is the obverse in channel flow and can be attributed to difference in the two geometries. The effect of Re_w and θ on u_s is also shown in Fig. 3.

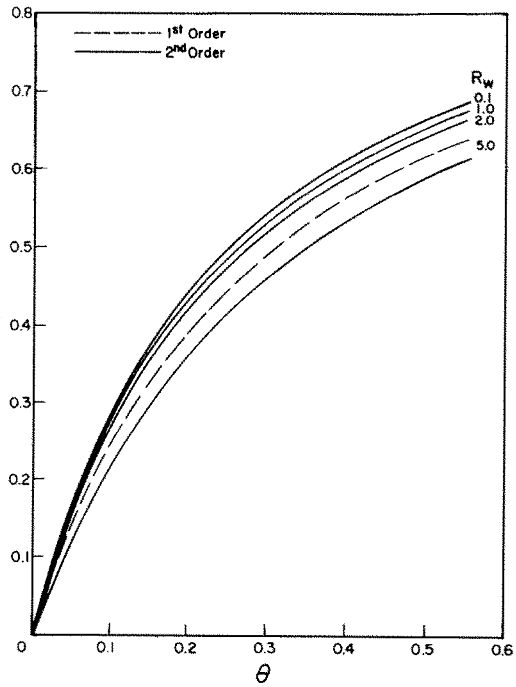

FIG. 3. First and second-order solutions of the effect of slip coefficient on normalized slip velocity for $Re_w = 0.1$, 1.0, 2.0 and 5.0.

Sparrow *et al.* [5] plotted a representative velocity profile with the value of Re_w equal to 2.0. Their numerical solution is compared with our perturbation solution in Fig. 2. The agreement is excellent lending support to the validity of the second-order perturbation solution. The first and second-order solutions are compared in Fig. 3 and in Table 1.

Table 1.

θ	Re_w	$u_s^{(1)} - u_s^{(2)}$
0.1	0.1	0
0.5		0
0.1	1.0	1.1×10^{-3}
0.5		1.2×10^{-3}
0.1	2.0	4.6×10^{-3}
0.5		4.7×10^{-3}
0.1	5.0	2.9×10^{-2}
0.5		3.0×10^{-2}

The values in column 3 of Table 1 are the difference in slip velocities between the first-order and second-order solutions. This difference increases with the value of Re_w. Except for Re_w equal to 5.0, the difference is satisfactorily small or negligible, suggesting the possibility of considering a higher-order solution for values of $Re_w > 2.0$. However, a value of Re_w of 5.0 is large for permeation flux in ultrafiltration membranes and would not be expected to be encountered. A higher-order solution then will not be considered.

4.2. *Concentration polarization*

Figures 4 and 5 show plots of concentration polarization similar to those of the channel flow system. Figure 4 is the plot for the no slip case ($\theta = 0$) with the normalized diffusion coefficient, $\alpha_1 = 0.1$, 0.2, 0.5, 1.0 and 2.0. Re_w is taken to be equal to 0.2. The agreement between this plot and that of Brian [2] is very satisfactory except for $\alpha_1 = 0.1$, which indicates a higher value of concentration polarization C_p. This is due to the effect of Re_w which was ignored by Brian but is not negligibly small for ultrafiltration systems. Comparison with

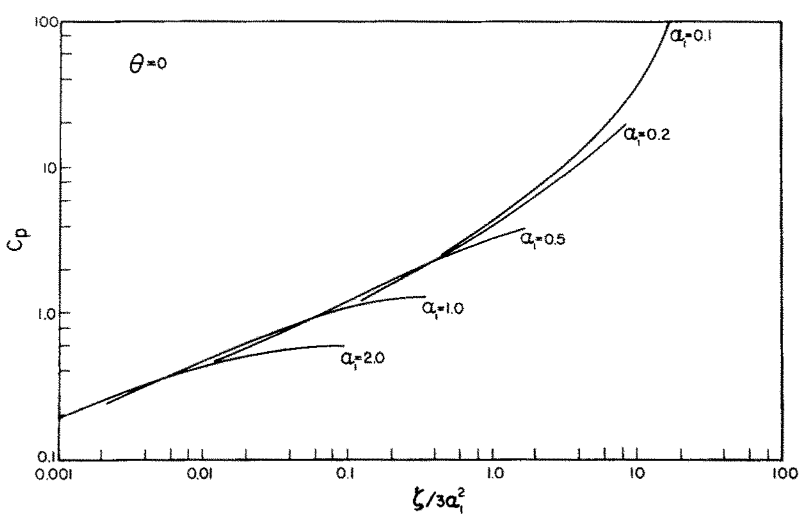

FIG. 4. Concentration polarization as a function of fraction of water removed (or longitudinal position) ζ, for $\theta = 0$.

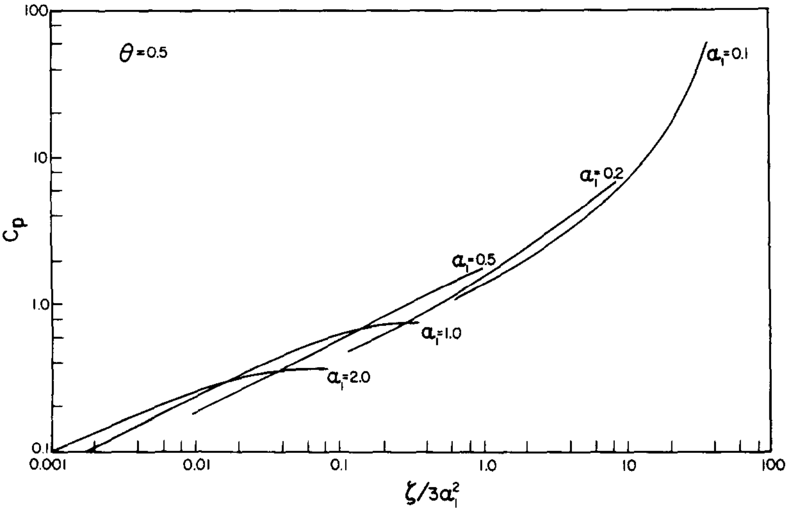

FIG. 5. Concentration polarization as a function of fraction of water removed (or longitudinal position) ζ, for $\theta = 0.5$.

Fig. 7 in the previous paper [4] shows that polarization is higher in tubular systems than in channel systems. This is so when the mean hydraulic radii are equal, that is, when the spacing of the flat membranes is one-half the diameter of the tubular membrane. However, when the spacing of the flat membranes is equal to the diameter of the tubular membrane, polarization will be greater for the flat membranes [note $\alpha_1 = D/v_w(r_w/2)$, $\alpha_0 = D/v_w h$]. For any value of α_1, C_p increases with the fraction of water removed ζ, and then levels out at an asymptotic value of C_p. The asymptote corresponds to the far-downstream solution for the polarization, and it is approached at relatively low values of ζ when α_1 is large. At low values of α_1, the asymptotic polarization is approached only as ζ is unity. When the value of C_p is substantially below the asymptotic value, the solution corresponds to the entrance region solution. The effect of slip is seen in Fig. 5. Comparing Figs. 4 and 5 it is seen that C_p decreases with increase in θ, the decrease being more significant when α_1 is small. These figures show a slight upward shift in the curves when $\theta = 0.5$ as compared to the case when $\theta = 0$, since, as the value of α_1 increases, the effect of θ is less pronounced. This phenomena is also observed in Fig. 6 and is discussed below.

In Fig. 6, $(C_p)\theta/(C_p)_{\theta=0}$ vs θ are plotted for $\alpha_1 = 0.1$, 0.2, 0.5, 1.0 and 2.0 when $\zeta = 0.10$ and 0.60. For any value of α_1, the normalized polarization is seen to decrease with increase in θ, and the decrease is more pronounced when α_1 is small. Thus, the reduction in polarization is nearly 10 times when $\alpha_1 = 0.1$ as compared to a 1.7 times reduction when $\alpha_1 = 2.0$ at $\theta = 0.5$ and $\zeta = 0.60$. It is seen that the effect of θ on C_p is similar to that of α_1. This phenomena, which has been discussed in detail by Singh and Laurence [4], shows that slip velocity enhances back diffusion of solutes from the membrane surface to the bulk solution, and thus reduces polarization.

When $\zeta = 0.10$, that is, when 10% of the water is removed, the normalized polarization has a lower value as compared to when $\zeta = 0.60$. When $\alpha_1 = 0.1$ and 0.2, however, the trend is reversed. This is because polarization for $\theta = 0$ is very large when $\zeta = 0.60$ as compared to when $\zeta = 0.10$, and α_1 due to its low value has little influence on reducing polarization.

5. CONCLUSIONS

The second-order perturbation solution of the velocity profiles agrees very well with the indirect numerical solution of other workers especially for $Re_w < 2.0$. The velocity profiles approach plug flow

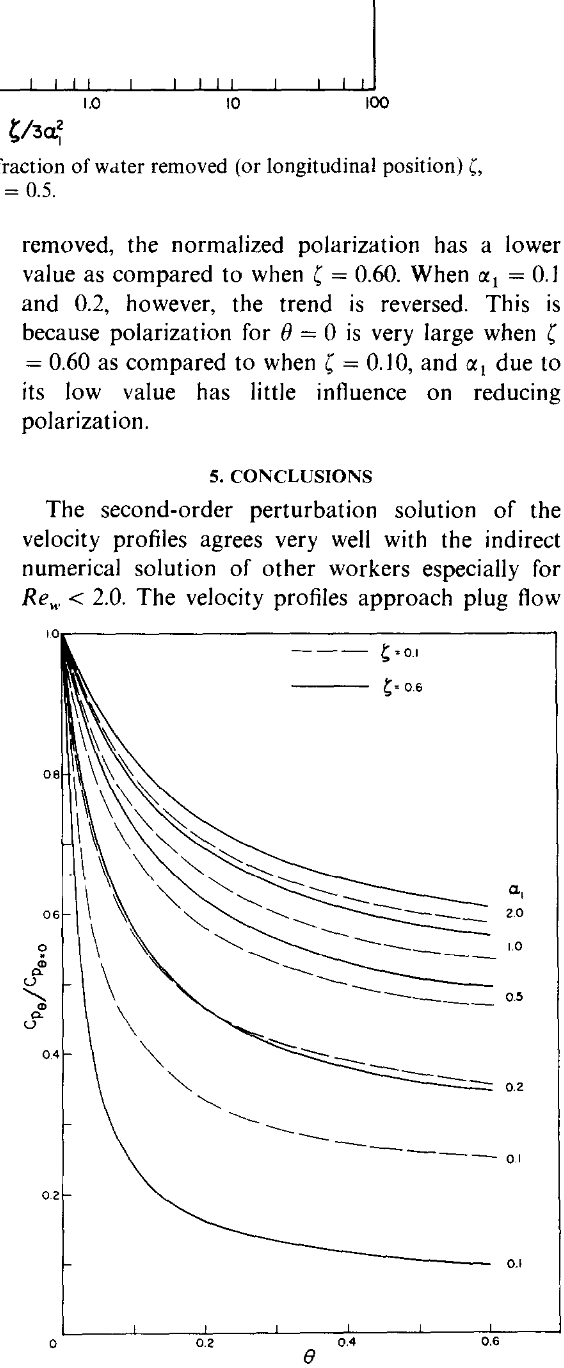

FIG. 6. Effect of slip coefficient on normalized concentration polarization.

with increase in the slip coefficient. The slip velocity increases with the slip coefficient and is seen to approach asymptotic value, and decreases with an increase in the wall Reynolds number. The finite difference solution of the diffusion equation is in very good agreement with the infinite-series solution of Brian. The effect of the slip coefficient on concentration polarization has been studied in detail. The polarization decreases with an increase in the slip coefficient. The effect is more significant for low values of the normalized diffusion coefficient indicating that the slip velocity enhances back-diffusion of solutes. The overall effect is to reduce polarization and increase flux rates through the membrane. As in the case of channel flow, the effect of the slip coefficient would be to decrease the magnitude of the pressure gradient due to the diminution in the shear stress at the membrane surface.

REFERENCES

1. W. F. Blatt, A. Dravid, A. S. Michaels and L. Nelson, Solute polarization and cake formation in membrane ultrafiltration: causes, consequences and control techniques, in *Membrane Science and Technology*, Edited by J. E. Flinn, p. 47. Plenum Press, New York (1970).
2. P. L. T. Brian, Mass transport in reverse osmosis, in *Desalination by Reverse Osmosis*, Edited by U. Merten, p. 161. M.I.T. Press, Cambridge, Mass. (1966).
3. D. von Rosenberg, *Methods for the Numerical Solution of Partial Differential Equations*, p. 22. Elsevier, New York (1969).
4. R. Singh and R. L. Laurence, Influence of slip velocity at a membrane surface on ultrafiltration performance—I. Channel flow system, *Int. J. Heat Mass Transfer* **22**, 721–729 (1979).
5. E. M. Sparrow, G. S. Beavers and L. Y. Hung, Channel and tube flows with surface mass transfer and velocity slip, *Physics Fluids* **14**(7), 1312–1319 (1971).

APPENDIX

(A) *Constants defined in equation* (33)

$$E = 1/(1+4\Theta),$$
$$M = 2(1+2\theta),$$
$$Q = 1/72(1+4\theta)^2,$$
$$G = 4(1+6\theta),$$
$$H = 9(1+4\theta),$$
$$P = 3M,$$
$$T = B/16(600),$$
$$B = 4QE,$$
$$H_1 = G_1 - 1621 - 10\,350\theta - 14\,400\theta^2,$$
$$G_1 = (2930 + 34\,920\theta + 135\,600\theta^2 + 172\,800\theta^3)E,$$
$$E_1 = 400(36\theta^2 + 30\theta + 5),$$
$$D_1 = 50H,$$
$$C_1 = 75(1+2\theta),$$
$$A_1 = 4.$$

(B) *The finite difference solution*

The diffusion equation (19), with the velocity field obtained from equations (34) and (35) is solved by a finite difference method implicit in η. A grid is chosen with $j = 1$ at $\eta = 0$ and so on as shown below:

$$\eta = 0,\quad \eta = \Delta\eta,\quad \eta = 2\Delta\eta,\ldots,\eta = 1,$$
$$j = 1,\quad j = 2,\quad j = 3,\ldots,j = NJ.$$

From above it can be seen that at $j = NJ$, $\eta = (NJ-1)\Delta\eta$. Similarly, at $\zeta = 0$, $m = 1$ and so on. $\Delta\zeta$ and $\Delta\eta$ are increments in the x and y directions.

The derivatives in equation (19) are replaced by finite difference analogues as shown below:

$$\left.\frac{\partial^2 C}{\partial \eta^2}\right|_{j,m} = \frac{C_{j+1,m} - 2C_{j,m} + C_{j-1,m}}{(\Delta\eta)^2}, \tag{B.1}$$

$$\left.\frac{\partial C}{\partial \eta}\right|_{j,m} = \frac{C_{j+1,m} - C_{j-1,m}}{2(\Delta\eta)}, \tag{B.2}$$

$$\left.\frac{\partial C}{\partial \zeta}\right|_{j,m} = \frac{C_{j,m} - C_{j,m-1}}{\Delta\zeta}. \tag{B.3}$$

Substituting equations (B.1)–(B.3) in equation (19) gives:

$$A_j C_{j-1,m} + B_j C_{j,m} + E_j C_{j+1,m} = F_j C_{j,m-1} = F_j, \quad \text{for } 2 \leqslant j \leqslant NJ-1, \tag{B.4}$$

where

$$A_j = \frac{-V\eta^{1/2} - \alpha_1}{2(\Delta\eta)} - \frac{\alpha_1 \eta}{(\Delta\eta)^2}, \tag{B.5}$$

$$B_j = \frac{U}{\Delta\zeta} + \frac{2\alpha_1\eta}{(\Delta\eta)^2}, \tag{B.6}$$

$$E_j = \frac{V\eta^{1/2} - \alpha_1}{2(\Delta\eta)} - \frac{\alpha_1 \eta}{(\Delta\eta)^2}, \tag{B.7}$$

$$F_j = \frac{U}{\Delta\zeta} C_{j,m-1}. \tag{B.8}$$

Using the Taylor series expansion around $j = 1$ and $j = NJ$, the boundary conditions, equations (21) and (22), can be written in finite difference form as:

$$C_{1,m} = \tfrac{4}{3}C_{2,m} - \tfrac{1}{3}C_{3,m}, \tag{B.9}$$

$$C_{NJ,m} = \frac{\alpha_1}{\{3\alpha_1 - 2(\Delta\eta)\}}\left[4C_{NJ-1,m} - C_{NJ-2,m}\right]. \tag{B.10}$$

The initial condition, equation (20) is replaced by

$$C_{j,m-1} = 1. \tag{B.11}$$

The above system of simultaneous equations can be represented by a tridiagonal coefficient matrix and is solved most efficiently by the method of Thomas [3]. The solution procedure has been outlined earlier [4]. The convergence of the numerical solution was found to be satisfactory for grid size of 0.05 for η and 0.001 for ζ.

INFLUENCE DE LA VITESSE DE GLISSEMENT, A LA SURFACE D'UNE MEMBRANE, SUR L'ULTRA-FILTRATION—2. SYSTEME D'ECOULEMENT EN TUBE

Résumé—L'effet de la vitesse de glissement sur la surface de la membrane est étudié en détail pour un système tubulaire de membrane. Une solution de perturbation au second ordre est trouvée satisfaisante. Les résultats sont comparés à ceux du canal reportés antérieurement. Comme dans le cas du système d'écoulement en canal, l'effet du coefficient de glissement sur la polarisation de concentration est identique à celui du nombre de Péclet: il augmente le transport par diffusion des molécules du soluté depuis la surface de la membrane jusqu'au coeur de la solution.

EINFLUSS DER SCHLUPFGESCHWINDIGKEIT AN EINER MEMBRANOBERFLÄCHE AUF DIE ULTRA-FILTRATIONSLEISTUNG II. SYSTEM MIT ROHRSTRÖMUNG

Zusammenfassung—Der Einfluß der Schlupfgeschwindigkeit an einer Membranoberfläche wurde ausführlich für ein System mit rohrförmiger Membran untersucht. Eine Lösung der Bewegungsgleichungen mittels Störgliedansatz zweiter Ordnung stellte sich als befriedigend heraus. Die Ergebnisse werden mit denjenigen für eine Kanalströmung verglichen, über die früher berichtet wurde. Wie im Fall der Kanalströmung ist der Einfluß des Schlupfkoeffizienten auf die Konzentrationspolarisation identisch dem der Peclet–Zahl, er vergrößert den Transport von gelösten Molekülen durch Diffusion von der Membranoberfläche in die Lösung.

ВЛИЯНИЕ СКОРОСТИ СКОЛЬЖЕНИЯ НА ПОВЕРХНОСТИ МЕМБРАНЫ НА УЛЬТРАФИЛЬТРАЦИЮ. 2. ТЕЧЕНИЕ В ТРУБЕ

Аннотация — Проведено детальное исследование влияния скорости скольжения на поверхности в системе трубчатых мембран на ультрафильтрацию. Найдено, что возмущенное решение уравнений движения второго порядка является весьма удовлетворительным. Результаты сравниваются с выводами, полученными для течения в канале в предыдущей работе. Как и в случае течения в канале, влияние коэффициента скольжения на распределение концентрации идентично влиянию числа Пекле, т. е. происходит усиление диффузионного переноса молекул растворенного вещества от поверхности мембраны в объём раствора.